

# Modelling cerebral haemodynamics: a move towards predictive surgery

Ed Long, CoMPLEx

Supervisors: Prof. Frank Smith & Mr. Neil Kitchen

Word count: 4622

March 9, 2007

---

Brain arteriovenous malformations are a relatively rare cerebrovascular defect which can lead to stroke. In planning treatment, the threat to a patient's health with no intervention must be weighed against the risks involved in the treatment: in the case of surgical intervention, this risk can be high.

There have been many attempts to model the dynamics of flow in the human circulation system. Flow characteristics such as the distribution of pressure or shear stresses can show where blood vessels are likely to rupture or conditions which might lead to reduced perfusion.

In this essay, I review results assessing the risks involved with surgical resection as a treatment for brain AVMs, introduce a selection of approaches to haemodynamic modelling and discuss whether simulating blood flow would be a useful and viable tool for surgical planning.

---

## Contents

<b>1</b>	<b>Medical background</b>	<b>1</b>
1.1	Cerebral circulation . . . . .	1
1.2	Imaging techniques . . . . .	1
1.3	Arteriovenous malformation . . . . .	2
<b>2</b>	<b>Treatment</b>	<b>4</b>
2.1	Treatment options . . . . .	4
2.2	Spetzler-Martin grading system . . . . .	4
2.3	Risk with no intervention . . . . .	5
<b>3</b>	<b>Modelling</b>	<b>5</b>
3.1	Elements of fluid mechanics . . . . .	5
3.2	Flow in blood vessels . . . . .	6
3.3	Flow on a vessel graph . . . . .	7
3.4	One-dimensional analysis . . . . .	8
3.5	Windkessel model . . . . .	9
<b>4</b>	<b>Discussion</b>	<b>10</b>

# 1 Medical background

## 1.1 Cerebral circulation

In order to function normally, the human brain requires a constant supply of oxygen-rich blood: roughly 20% of the body's blood and 25% of its oxygen [10]. This must perfuse fully through the convoluted structure of the cortex. Although neurons will still function when perfusion is as low as 33% of its optimal level, a drop to 20% typically results in cell death [3]: in the case of brain cells such damage is irreversible.

The proximity of the cells of the brain to the larger blood vessels also constitutes a risk in that weakening of or damage to the blood vessel walls can lead to ballooning (*aneurysm*) or rupture of the blood vessels, creating a rise in pressure which also damages the cortex.

Injury to the brain in the manner described above can result in *stroke*. In the former case, where the damage is caused by starvation of oxygen, it is termed *ischaemic stroke*. Damage by bleeding into the brain is termed *haemorrhagic stroke* [24].

Blood supply to the brain is via four large arteries: the left and right *internal carotid* and *vertebral* arteries. The former supply the forebrain and eyes, while the latter supply the mid- and hindbrain. Of the total blood supply to the brain, about 80% is carried by the two carotid arteries [24]. Within the head, these four arteries are connected by a network of blood vessels called the *circle of Willis*—see Figure 1, which allows blood to be redistributed if the supply is reduced from a particular artery and balances the pressure in the arterial system.

As the arteries are stretched over bones, nerves and membranes in the neck, extreme head movement can cause obstruction of one or two arteries, so one part of the brain may 'steal' blood from another via the circle of Willis to compensate [3]. It should, however, be noted that since the communicating vessels are often much narrower than the main supply arteries, the system cannot compensate for the complete blockage of these vessels [24]. Indeed, a number of people lack one of the communicating arteries, putting them at greater risk of brain damage in the case of reduced supply.

The major arteries then branch into smaller *arterioles* and then into the beds of fine *capillaries* where various substances (oxygen, carbon dioxide, ethanol, certain hormones, glucose and certain amino acids) may pass between the bloodstream and the neurons.

## 1.2 Imaging techniques

Techniques used to produce images of vasculature in the head are varied. The 'gold standard' for defining arterial and venous anatomy, according to [15], is using *arteriography* (or *angiography*) in which a radiocontrast agent is administered into the area of interest, allowing the vasculature to be imaged with X-rays. Combination of radiocontrast X-ray imaging with computed tomography (CT) technology allows a three-dimensional image of the vasculature to be rendered.

Recent papers [8] advocate the use of *scintigraphy* in which an unstable element called a *radionuclide* is administered and its course is monitored using a camera which detects gamma ray emissions. Radionuclides cited in the literature include Technetium-99m [8] and Xenon-133 [27].

Magnetic Resonance Imaging (MRI) can also be used to image blood vessels. The contrast can be increased by injecting a paramagnetic agent such as gadolinium into the bloodstream. MRI also allows the measurement of the blood's velocity within the veins and arteries and does not expose the patient to X-ray radiation as in an angiogram or CT scan.

Another technology which can be used to monitor blood flow velocity is *transcranial Doppler ultrasonography* (TCD). This uses a small hand-held device (*transducer*) which emits and detects high frequency soundwaves; different velocities in the image are displayed in real time on a computer screen. Again,

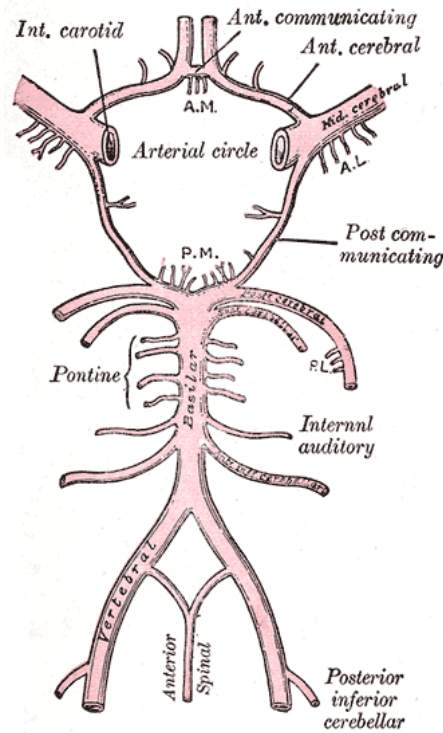


Figure 1: The circle of Willis (from *Gray's Anatomy*)

there is no radiation dose and the equipment is much less bulky than in MRI so this type of imaging is suitable for monitoring flow dynamics during surgery.

As a final aside, corrosion casting of cadavers produces three-dimensional casts of the vasculature which can be a valuable resource in study of vascular anatomy, although it is clearly not a useful method as a patient-specific diagnostic aid. A resin is injected into the blood vessels of interest which slowly solidifies leaving a cast of the veins and arteries in their correct positions relative to the bones. A more detailed description of the process is found in [3], chapter 15.

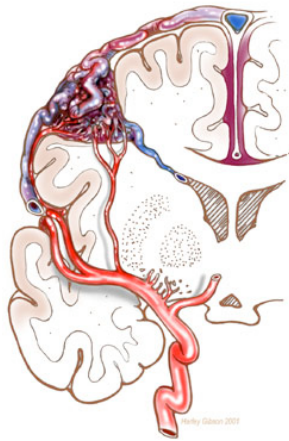
### 1.3 Arteriovenous malformation

An *arteriovenous malformation* (AVM) is a defect of the circulation system [14] in which, instead of filtering through a capillary bed, blood flows at high pressure directly from a feeding artery, through a network of relatively wide vessels into the draining veins (a process termed *shunt*) [5]. This puts a higher stress on the blood vessels and also prevents oxygen and nutrients in the bloodstream from being passed onto the tissues.

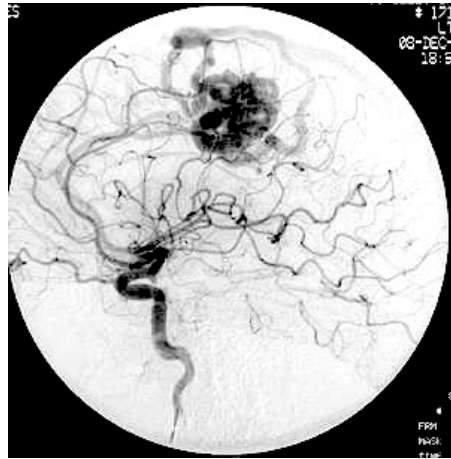
The anatomy of the AVM comprises the feeding arteries, which may be one or many; the draining veins; and the short-circuit in between, which is termed a *fistula*. In many cases there is also a complex tangle of vessels present called a *nidus*.

This essay will concentrate on AVMs located in the brain (often abbreviated as BAVMs) as these occur most commonly and are most likely to be damaging to health. Although symptoms are only seen in an estimated 12% of persons with AVMs, they can be severe and include headaches, seizures, muscle weakness, paralysis, tingling, memory loss and hallucination among others. The specific symptom is dependent on the position of the malformation in the brain. See Figure 2 for pictures of AVMs<sup>1</sup>.

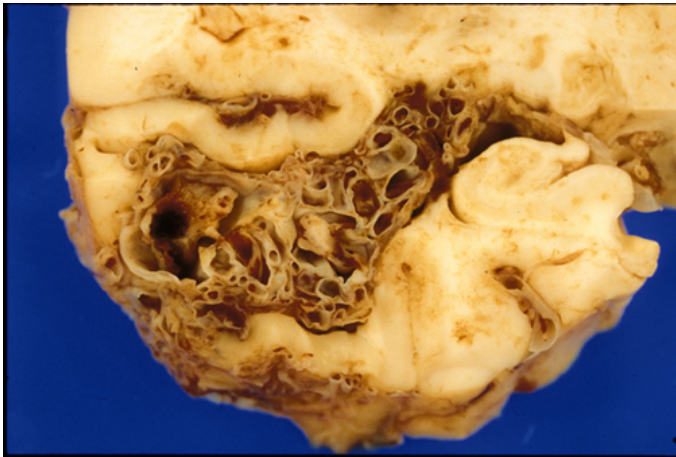
<sup>1</sup>Picture credits: Figure 2(a) <http://www.neurosurgery.ufl.edu/Patients/avm.html>, (b) <http://www.thecni.org/stroke/surgery.htm>, (c) [http://missinglink.ucsf.edu/lm/ids\\_104\\_cerebrovasc\\_neuropath/Case2/Case2PathologyGross.htm](http://missinglink.ucsf.edu/lm/ids_104_cerebrovasc_neuropath/Case2/Case2PathologyGross.htm) and (d) <http://www.ispub.com/ostia/index.php?xmlFilePath=journals/ijra/vol4n2/avm.xml>



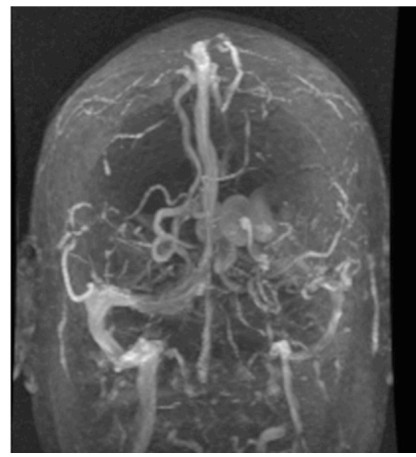
(a) Diagram of an AVM



(b) An AVM visible in an angiogram



(c) A coronal slice through a brain with a large AVM



(d) Three-dimensional rendering of a magnetic resonance angiogram

Figure 2: Images of arteriovenous malformations

AVMs may occur deep within the brain or superficially. Fistulas may also be found within the *dura mater*; the tough, outermost membrane surrounding the brain.

The greatest threat to health is the potential of haemorrhage, which is a risk in AVMs as the walls of the arteries are often weakened. The risk of haemorrhage from an AVM is roughly 2% each year [5][14] although haemorrhage has a relatively high chance of causing death (20%) or disability (30%) [5]. AVMs are most frequently discovered in patients presenting with haemorrhagic stroke (around half of all newly discovered AVMs), while a large number are detected 'incidentally' (ie. without directly related symptoms) or in patients presenting with epileptic seizure [5]. Presentation with stroke is also at an unusually young age—the average age is 40.

AVMs are believed to be congenital (present at birth) although dural fistulas may form as a result of injury [5]. Also, the stress of the increased blood pressure can lead to further malformation and weakening of the blood vessels so they become more of a risk as time goes on. There is not believed to be a genetic cause.

Characteristic	Points
Size of AVM	
Small (<3cm)	1
Medium (3–6cm)	2
Large (>6cm)	3
Adjacent brain	
Non-eloquent	0
Eloquent	1
Venous drainage	
Superficial	0
Deep	1

Table 1: The Spetzler-Martin grading system

## 2 Treatment

### 2.1 Treatment options

Although the majority of AVMs do not pose an immediate threat to health, treatment is necessary in cases where there is a risk of rupture or where symptoms have already been expressed.

Three common treatments are *microsurgery* (resection or clipping), *embolisation* (injection of an *embolic agent* into the affected blood vessels which occludes blood flow) or *radiosurgery* (obliteration of the malformation using a beam of gamma or X-rays focused on the site of the AVM [26]). Papers refer frequently to a *management strategy* for treating AVMs rather than a single therapy.

Surgery is the only treatment which, if successful, immediately removes the risk of haemorrhage. Embolisation may provide immediate reduction in blood supply to the AVM but is rarely curative when used as a primary treatment. Used before microsurgery it can make surgical treatment safer. Embolic agents include ethanol, a type of glue (*cianoacrylate*) or small metal coils which induce thrombosis. Radiosurgery avoids open surgery but is less effective and takes two years for the malformation to be obliterated, so this treatment is unsuitable when there is a present threat to health [13].

In [12], Nakaji *et al.* stress that the risks of intervention must be weighed against the risk from the malformation itself. They also note that the diagnostic methods mentioned above carry their own risks (exposure to radiation, injection of contrast agents), which must also be taken into account as part of a treatment plan.

Surgical treatment, particularly, carries a high risk of neurological deficit. In a study by Hartmann *et al.* [6], 41% of patients in a group of 124 showed new neurological deficits immediately after microsurgical resection; 15% were classified as disabling. In long-term follow up, however, these percentages dropped to 38% and 6% respectively.

### 2.2 Spetzler-Martin grading system

The risks involved with surgical resection are roughly quantified by a guideline proposed in 1986 by Spetzler and Martin in [21]. In this scheme, cases where surgical resection would be considered risky are those where the malformation is large; positioned in an *eloquent* brain region (responsible for sensation, motor control, language, vision among others); and with deep venous drainage. The points are awarded according to Table 1.

Summation of the points gives a score of between I and V, where cases graded I are most likely to be successfully treated with surgery and cases graded V are least likely. In [15], Ogilvy *et al.* note that there was low morbidity after surgical resection in patients graded with I, II or III points but that treatment-associated morbidity was as high as 31.2% in patients with grade IV lesions and 50% with grade V. They recommended surgery for all patients with grade I and II lesions; further analysis before the decision

on patients with grade III lesions and to seek a multidisciplinary approach on patients presenting with Spetzler-Martin grade IV or V. The report also noted that, although the grading system was designed to predict surgical outcome only, deterioration due to combined treatments was also strongly indicated by a high Spetzler-Martin score.

In the Hartmann *et al.* study, neurological deficit was strongly linked with Spetzler-Martin grade. The paper also mentioned that female patients were more likely to develop neurological deficits after surgical resection.

### 2.3 Risk with no intervention

The relative risk of haemorrhage with no intervention is less well documented. The strongest indicator that an AVM will bleed is if it has bled in the past (annual risk of haemorrhage rises to 17.8% according to Mast *et al.* [9]). A study in 2000 [22] found significant increased risk with small AVM size, deep venous drainage and the presence of feeding-artery or intranidal aneurysms, and a reduced risk associated with AVMs positioned in so-called *arterial borderzones*: AVMs fed by two or more major circle of Willis arteries.

A clinical trial (ARUBA [11]) is currently underway to assess the need for intervention in AVMs detected before any haemorrhage has occurred. Based on data collected so far, they found that intervention in unbled AVMs led to an increased chance of haemorrhage over a five year course (4.2% untreated compared with 17.3% treated). They also noted that spontaneous bleeding of untreated AVMs were associated with milder clinical syndromes than bleeding of treated AVMs.

The age of the patient must also be taken into account. Given that there is a small chance of haemorrhage occurring each year, the cumulative probability of haemorrhage occurring over a patient's remaining natural history is higher for a younger patient than an elderly one. For this reason, intervention (surgical or otherwise) may be more appropriate when the patient is relatively young.

## 3 Modelling

### 3.1 Elements of fluid mechanics

The physical principles governing fluid flows are similar to those governing the mechanics of solids: namely conservation of mass, momentum and energy. Fluids are distinguished from solids by the fact that they continuously deform under an applied shear stress. A second point is that, in fluid dynamics, equations usually describe the rate of change of velocity, density *etc.* at a fixed point (the *Eulerian* description) rather than following a fluid particle (the *Lagrangian* description).

Flows can be divided generally into categories depending on whether or not they are compressible or incompressible; viscous or inviscid; and laminar or turbulent. Liquids are normally assumed to be incompressible, whereas gases are compressible. In a three-dimensional flow with components of velocity  $(u, v, w)$ , mass conservation requires that an incompressible flow satisfies:

$$\frac{\partial u}{\partial x} + \frac{\partial v}{\partial y} + \frac{\partial w}{\partial z} = 0 \quad (1)$$

Conservation of momentum is given by a set of equations named after Claude-Louis Navier and George Gabriel Stokes:

$$\frac{\partial u}{\partial t} + u \frac{\partial u}{\partial x} + v \frac{\partial u}{\partial y} + w \frac{\partial u}{\partial z} = F_x - \frac{1}{\rho} \frac{\partial p}{\partial x} + \nu \nabla^2 u \quad (2)$$

$$\frac{\partial v}{\partial t} + u \frac{\partial v}{\partial x} + v \frac{\partial v}{\partial y} + w \frac{\partial v}{\partial z} = F_y - \frac{1}{\rho} \frac{\partial p}{\partial y} + \nu \nabla^2 v \quad (3)$$

$$\frac{\partial w}{\partial t} + u \frac{\partial w}{\partial x} + v \frac{\partial w}{\partial y} + w \frac{\partial w}{\partial z} = F_z - \frac{1}{\rho} \frac{\partial p}{\partial z} + \nu \nabla^2 w \quad (4)$$

Here  $\rho$  is the density of the fluid,  $p$  is the pressure,  $\nu$  is the *kinematic viscosity* and  $F_{x,y,z}$  denote components of body forces acting on a fluid element in the respective directions.

More specific results can be obtained if we define boundary conditions for the flow: the vessel in which it is flowing as well as what forces and pressures are acting on it. Consider an incompressible flow in a rigid, horizontal tube of radius  $a$ , which lies along the  $x$ -axis. We shall assume that the fluid can flow only along the direction of the tube so  $v$  and  $w$  are zero. We also require  $u = 0$  on the boundaries of the tube (no slip) and ignore the body forces due to gravity. Solving the Navier-Stokes equations for these conditions, as detailed in [4], gives:

$$u = -\frac{1}{2\mu}(a^2 - y^2)\frac{dp}{dx} \quad (5)$$

in the case of a two-dimensional flow (flow in a channel) or:

$$u = -\frac{1}{4\mu}(a^2 - r^2)\frac{dp}{dx} \quad (6)$$

in three-dimensional flow through a tube, where  $r = \sqrt{y^2 + z^2}$ .

Integration of the above result gives the rate of flow  $\frac{dQ}{dt}$  as:

$$\frac{dQ}{dt} = 2\pi \int_0^a u r dr = -2\pi \int_0^a \frac{r}{4\mu}(a^2 - r^2)\frac{dp}{dx} dr \quad (7)$$

$$= -\frac{\pi a^4}{8\mu} \frac{dp}{dx} \quad (8)$$

The *Reynolds number*:

$$Re = \frac{\rho u L}{\mu} \quad (9)$$

is a dimensionless measurement of local flow characteristics.  $L$  denotes the *characteristic length*, which is the vessel diameter in the case of a tube of circular cross section. Depending on the vessel containing the flow, it can be used to indicate the point at which a laminar flow becomes turbulent. In circular tubes, the critical value for  $Re$  where turbulent flow may occur is around 2300.

### 3.2 Flow in blood vessels

Blood may, to some extent, be modelled as a classical fluid but it should be noted that its structure is much more complex: a suspension of red and white blood cells and cell fragments (*platelets*) in a liquid medium (*plasma*) which also contains various proteins and electrolytes in solution. Study of the dynamics of blood in this context is called *haemorheology*, though I shall consider only continuum models in this essay.

The branching and narrowing of the arterial system also means that the Reynolds number (and hence the flow characteristics) varies widely throughout the system; from over 3000 in the aorta to around 0.002 in the capillaries.

Recall that AVMs are abnormal owing to their lack of a capillary bed: the vessels are wide along the whole length and so the Reynolds number of the flow is atypically high. They also commonly feature a large number of branchings from one or several *mother vessels* into a number of *daughters*.

Simulation of blood flow can be achieved by direct numerical solution of the governing equations described above on a discrete mesh. Numerical methods used include finite element, finite difference or finite volume schemes. Direct simulation in this manner may agree well with real measurements but is computationally intensive and does little to help understand the characteristics of the problem.

Attempts to model the flow analytically give more information on the characteristics of the flow, though numerical methods must be employed at some point in the process. Approaches to modelling high

Reynolds number flows around branching vessels, as would be seen in AVMs, is seen in Smith *et al.* in [18], [19] and [20] and in Bowles *et al.* in [1]. In [20], Smith *et al.* describe methods whereby wall shapes around a branching point are specified by explicit functions. They report a close agreement between the flow rates calculated using their models and direct numerical simulation.

Useful results may also be obtained in simplified models, considering flows in only one dimension, this simplification allows study of more complex networks without becoming computationally intractable. In the next three sections I introduce papers which address blood flow in arterial networks using one- or zero-dimensional methods.

### 3.3 Flow on a vessel graph

In [2], the approach of Bunicheva *et al.* to modelling branching flows is to treat the circulatory system as a network of nodes and one-dimensional edges instead of attempting to understand the particular geometry of a single branching. This makes it much simpler to assess flow properties on a wider scale: for example in a complex structure like an AVM; the whole cranial circulation system; or indeed whole-body circulation study.

The veins and arteries of interest are used as edges of the graph and the nodes are divided into three categories: *branching points*, *capillary beds* and *boundary points* (the points where flow either enters or leaves the system).

The equations of motion are solved on the edges of the graph and there are additional constraints which must be satisfied for each particular boundary point.

Firstly, it is assumed that flow,  $u(x, t)$ , is one-dimensional through a tube of variable cross-section  $S(x, t)$ , so the mass conservation equation becomes:

$$\frac{\partial S}{\partial t} + \frac{\partial}{\partial x}(uS) = 0 \quad (10)$$

For conservation of momentum we have:

$$\frac{\partial u}{\partial t} + \frac{\partial}{\partial x}\left(\frac{u^2}{2}\right) = -\frac{1}{\rho}\frac{\partial p}{\partial x} - \frac{8\pi\nu u}{S} \quad (11)$$

The authors assume that the vessels have a maximum and minimum cross-section and that it varies linearly with pressure between these two values. ie.

$$S(p) = S_{min} + \theta(p - p_{min}), \text{ where } \theta = \frac{S_{max} - S_{min}}{p_{max} - p_{min}} \quad (12)$$

and  $p_{max}$  and  $p_{min}$  are the corresponding pressure at which the vessel has cross-sectional area  $S_{max}$  or  $S_{min}$  respectively.

The constraints at the nodes of the graph are as follows:

At a branching point where an incident edge  $i$  has flow velocity  $u_i$  and cross-sectional area  $S_i$  at its endpoint, assign a coefficient  $z_i = 1$  for flow into the node and  $z_i = -1$  for flow issuing from it. Then impose the constraints:

$$\sum_i z_i u_i S_i = 0 \quad (13)$$

$$\frac{u_i^2}{2} + \frac{p_i}{\rho} = \frac{u_j^2}{2} + \frac{p_j}{\rho}, \quad i \neq j \quad (14)$$

For a flow passing through a capillary bed we have the conditions:

$$z_i u_i S_i + z_j u_j S_j = 0 \quad (15)$$

$$z_i u_i S_i = k_d(p_i - p_j), \quad (16)$$

where  $k_d$  is a constant (*Darcy's filtration coefficient*) relating flow velocity to hydraulic gradient.

Finally, for the node at the beginning of the network we set a function  $q(t)$  giving the initial input flow, for example the output of the heart if it is the beginning of our network. Bunicheva *et al.* give a function for heart output flow as:

$$q(q_{max}, q_{min}, \tau_S, \tau_P) = \begin{cases} q_{max} - \frac{1}{\tau_S^2}(q_{max} - q_{min})(t - \tau_S)^2 & \text{if } 0 \leq t \leq \tau_S \\ q_{min} & \text{if } \tau_S \leq t \leq \tau_P \end{cases} \quad (17)$$

Implementation of this model showed close agreement with direct numerical simulation and analytical solution in calculating the pressure drop on a specified elastic vessel.

### 3.4 One-dimensional analysis

A similar mathematical formulation is taken by Steele *et al.* in [23] from the Stanford University Engineering department under Charles Taylor. Instead of velocity  $u$ , Steele uses volumetric flow rate  $Q$  as a primary variable alongside the cross-sectional area  $S$  and pressure  $p$ .

This gives the equations for conservation of mass and momentum as:

$$\frac{\partial S}{\partial t} + \frac{\partial Q}{\partial x} = 0 \quad \text{and} \quad (18)$$

$$\frac{\partial Q}{\partial t} + \frac{\partial}{\partial x} \left( (1 + \delta) \frac{Q^2}{S} \right) + \frac{S}{\rho} \frac{\partial p}{\partial x} = N \frac{Q}{S} + \nu \frac{\partial^2 Q}{\partial x^2} \quad (19)$$

where  $\delta$ , a term related to the profile function of the velocity, is taken to be  $\frac{1}{3}$  and  $N$ , a viscous loss term, is taken as  $-8\pi\nu$ .

Instead of a linear relationship, as used above, the pressure and cross-sectional area of the vessel are related by the formula:

$$p(S, x, t) = p_0 + \frac{4}{3} \frac{Eh}{r_0(x)} \left( 1 - \sqrt{\frac{S_0(x)}{S(x, t)}} \right) \quad (20)$$

taken from [16], where  $E$  is the Young's modulus,  $h$  is the thickness of the vessel wall,  $r_0$  is the vessel radius at a reference pressure  $p_0$  and  $S_0$  is the cross sectional area of the vessel at time  $t = 0$ . We further have:

$$\frac{Eh}{r_0(x)} = k_1 e^{k_2 r_0(x)} + k_3 \quad (21)$$

where the constants  $k_i$  are determined by fitting to experimental data.

The paper also describes how energy loss coefficients are calculated to take into account flow around stenoses and diverging or converging flow bifurcations.

The model described above was used to predict flow rate in a graft used to bypass an artificial stenosis in the thoracic aorta of a group of pigs. The dynamic equations were solved using a one-dimensional finite element approach and the error in the predicted flow was at most 10.6%, with an average of 4.2% error. There was also good qualitative agreement between the predicted and measured flow patterns.

The *in vivo* blood flow distribution was measured using phase-contrast magnetic resonance angiography, pressure was measured using catheters placed in the aorta and the geometry of the blood vessels was determined using three-dimensional contrast-enhanced magnetic resonance angiography in order to construct the case-specific models used in the simulations.

### 3.5 Windkessel model

In [17], Olufsen *et al.* employ a *three-element windkessel model*—an analogue of part of the arterial system using electrical circuit components—to model pressure regulation in pulsatile arterial flow. The model featured in the article used two resistors and a capacitor, as shown in Figure 3, to represent flow in the middle cerebral artery. The resistor  $R_S$  represents the systemic resistance to flow in arteries leading to the middle cerebral artery, the capacitor  $C_S$  represents the systemic *compliance*—the resistance of a vessel to deforming in response to pressure, and the second resistor  $R_P$  represents resistance due to the cerebrovascular bed.

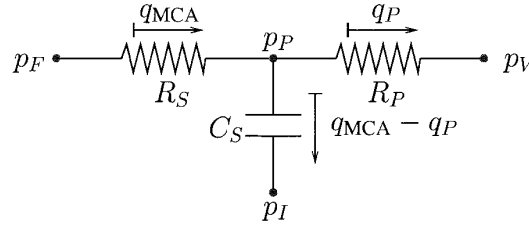


Figure 3: The three-element windkessel model. Figure from Olufsen *et al.*, 2002.

The model uses an *in vivo* measurement of blood pressure taken in the finger as an input, shown as  $p_F$  in the diagram and the output is the flow rate in the middle cerebral artery  $q_{MCA}$ . Other parameters listed in the diagram are the flow rate and pressure in the cerebrovascular bed,  $q_P$  and  $p_P$ ; the venous pressure  $p_V$  and the intracranial pressure  $p_I$ .

Pressure and flow rates are assumed to be sums of harmonic functions of the form:

$$p(t) = Pe^{i\omega t} \quad \text{and} \quad q(t) = Qe^{i\omega t} \quad (22)$$

where  $P$  and  $Q$  are pressure and flow in the frequency domain. Over this domain, we may write equations relating the pressure and flow in the circuit as:

$$P_F - P_P = R_S Q_{MCA} \quad (23)$$

$$P_P - P_V = R_P Q_P \quad (24)$$

$$P_P - P_I = \frac{Q_{MCA} - Q_P}{i\omega C_S} \quad (25)$$

The functions over the frequency and time domains are related by the usual Fourier series representation, namely:

$$p(t) = \sum_{k=-\infty}^{\infty} P(\omega_k) e^{i\omega_k t} \quad (26)$$

$$q(t) = \sum_{k=-\infty}^{\infty} Q(\omega_k) e^{i\omega_k t} \quad (27)$$

$$P(\omega_k) = \frac{1}{T} \int_{-T/2}^{T/2} p(t) e^{i\omega_k t} dt \quad (28)$$

$$Q(\omega_k) = \frac{1}{T} \int_{-T/2}^{T/2} q(t) e^{i\omega_k t} dt \quad (29)$$

From this we may obtain the ordinary differential equation:

$$R_S \left[ \frac{dq_{MCA}}{dt} + \frac{(R_S + R_P)q_{MCA}}{C_S R_S R_P} \right] = \frac{dp_F}{dt} + \frac{p_F}{C_S R_P} \quad (30)$$

which, given  $p_F$  (the pressure in the finger), can be integrated to give  $q_{MCA}$  as a function of time.

Olufsen *et al.* used the model to compute pressure and flow variation in a subject as they moved from a seated to a standing position. The pressure and flow at first both drop and then return to normal over a 20 second period. The computed results agreed well with measurements both over the 100 second timecourse (see Figure 4) and on a beat-to-beat basis.

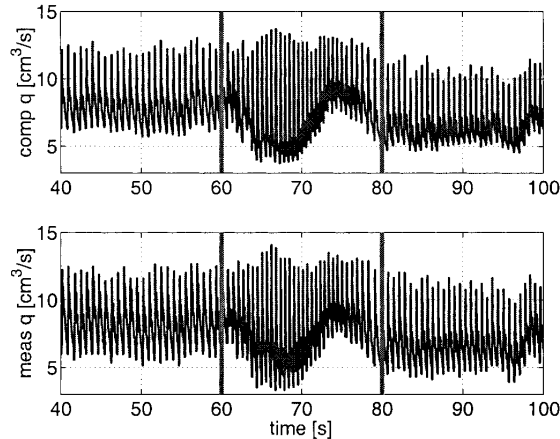


Figure 4: Computed (top) and measured (bottom) flow over a 100 second timecourse. The patient stands at 60s. Figure from Olufsen *et al.*, 2002

## 4 Discussion

Advances in technology give surgeons access to increasingly detailed diagnostic information on a patient's present condition. This means greater potential to make advantageous decisions on treatment. The wide range of data can, however, be a confounding factor through sheer volume of information or in the case that if different characteristics of the presentation contradict one another with respect to treatment.

Current surgical planning is, in the main, based on the empirical data from previous cases and the personal experience of the surgeon. Whilst more detailed statistical analysis of factors contributing to risk can differentiate cases into a greater and greater number of subcategories, individual variation means this consideration cannot be truly patient specific.

Arteriovenous malformations are a clear example where there exist a multitude of factors contributing to the risks involved in treatment or nonintervention. Using modelling to obtain patient-specific haemodynamic information could be a valuable tool for assessing the outcome of surgery (and potentially other treatments) as well as the risk of haemorrhage if an AVM is left untreated.

Using computer modelling techniques as an aid to planning has long been widespread in disciplines such as design, engineering and manufacturing, so what potential does it have in a medical context?

A first application is three-dimensional rendering of patient-specific anatomy. Kikinis *et al.* [7] describe reconstructing anatomically complex structures from MRI data in a number of case studies including a frontoparietal AVM. The authors reported that the model permitted more detailed study of the surface topology and adjoining vessels, allowing the surgeons to minimise the size of the craniotomy and damage to the surrounding brain.

In the case of vascular surgery, a second level would be calculating patient-specific blood flow in the

geometry reconstructed as described above. In [25], Taylor *et al.* describe use of a developmental software package called ASPIRE which combines these two functions as well as featuring an interactive treatment-planning ‘sketchpad’ in which angioplasty or arterial bypasses can be performed on the model.

The paper recounted a mock clinical case in 1998 where the patient had complete occlusion of the right iliac and left superficial femoral artery and a 50% reduction in diameter of the left iliac and right superficial femoral artery. The authors described three possible treatment plans: an aorto-femoral bypass graft with proximal end-to-side anastomosis; the same graft with proximal end-to-end anastomosis and a balloon angioplasty in the left common iliac artery with a femoral-to-femoral bypass graft (see Figure 5).



Figure 5: Three-dimensional rendering of the arteries and three possible treatment plans. Grafts are shown in white. Figure from Taylor *et al.*, 1999

Numerical simulation of the haemodynamics using an automatically generated finite-element mesh showed that pressure losses were lowest in the first of the three treatment plans, suggesting that this graft would be the most appropriate treatment.

Despite the encouraging results, there are a large number of considerations which must be addressed in using modelling in this context: Taylor *et al.* acknowledged that the simulations mentioned in their paper were “crude compared to the true complexity and elegance of human function”. Assumptions included treating the blood as a Newtonian fluid and the blood vessels as rigid tubes, which the authors hoped could be amended in future versions.

Secondly, time is an important factor: the calculations involved in the implementation of the above procedure took 20 hours per analysis. Improvement in computer processor design since 1998 will of course make quicker and more complex analysis possible. The authors noted that the time period between acquisition of imaging data and the operation would usually exceed 20 hours but suggested a maximum run time of 1–2 hours as feasible for use in clinical planning.

Financial considerations must be taken into account. In Kikinis *et al.* [7], the system used to render three-dimensional images of brain anatomy had to be operated by a specially-trained technician un-

der the supervision of a neuroradiologist: paying these two specialists would be expensive and, in comments on the paper, there were doubts that it would be affordable. Automation of the model construction as much as possible as well as a design that is operable by those without specialist technical training would be necessary to avoid these additional costs.

The lack of clear data on risk associated with an AVM diagnosis, particularly in unbled cases, and the extensive patient to patient variation is a barrier to giving clear advice on treatment. A detailed statistical analysis of the ARUBA study, amongst others, should make a significant difference in tackling this problem. In addition, combining empirical data with deterministic models has the potential to add another string to the surgeon's bow, though treatment decisions must also take into account clinical guidelines and the wishes of the patient and their family. As well as relatively computationally-intensive numerical simulations such as used in [25], simpler models such as those mentioned in sections 3.3, 3.4 and 3.5 have shown to give useful results, close to direct simulation or *in vivo* measurements. With regard to planning AVM resection specifically, the model would be required to maximise the accuracy of critical parameters such as pressure variation and shear stresses subject to the constraints of time, cost and ease of use.

In conclusion, the tools for producing accurate and clinically relevant haemodynamic models are already available but must conform to the standards discussed above before they could be used in a clinical environment. If these standards can be met then rigorous clinical testing could validate the benefit of adopting a paradigm of predictive medicine as an additional facet of surgical planning.

## References

- [1] R.I. Bowles, S.C.R. Dennis, R. Purvis, and F.T. Smith. Multi-branching flows from one mother tube to many daughters or to a network. *Phil. Trans. R. Soc. A*, 363:1045–1055, 2005.
- [2] A. Ya. Bunicheva, S.I. Mukhin, N.V. Sosnin, and A.P. Favorskii. An averaged nonlinear model of hemodynamics on the vessel graph. *Differential Equations*, 37(7):949–956, 2001.
- [3] Andrew L. Carney and Evelyn M. Anderson, editors. *Advances in Neurology*, volume 30. Raven Press, 1981.
- [4] Y.C. Fung. *Biodynamics: Circulation*. Springer-Verlag, 1984.
- [5] Jan Harrington. AVM Support UK. <http://www.avmsupport.org.uk/index.php>.
- [6] A. Hartmann, C. Stapf, C. Hofmeister, J.P. Mohr, R.R. Sciacca, B.M. Stein, A. Faulstich, and H. Mast. Determinants of neurological outcome after surgery for brain arteriovenous malformation. *Stroke*, 31:2361–2364, 2000.
- [7] Ron Kikinis, P. Langham Gleason, Thomas Moriarty, Matthew Moore, Eben Alexander, Philip E. Stieg, Mitsunori Matsumae, William E. Lorensen, Harvey E. Cline, Peter M. Black, and Ferenc Jolesz. Computer-assisted interactive three-dimensional planning for neurosurgical procedures. *Neurosurgery Online*, 38(4), 1996.
- [8] Byung-Boong Lee, Y.S. Do, Wayne Yakes, D.I. Kim, Raul Mattassi, and W.S. Hyon. Management of arteriovenous malformations: A multidisciplinary approach. *Journal of Vascular Surgery*, 39(3):590–600, 2004.
- [9] Henning Mast, William L. Young, Hans-Christian Koennecke, Robert R Sciacca, Andrei Osipov, John Pile-Spellman, Lotfi Hacein-Bey, Hoang Duong, Bennett M. Stein, and J.P. Mohr. Risk of spontaneous haemorrhage after diagnosis of cerebral arteriovenous malformation. *The Lancet*, 350:1065–1068, 1997.
- [10] Patrick McCaffrey. Neuroanatomy of speech, swallowing and language: Unit 11. The Blood Supply, California State University. <http://www.csuchico.edu/~pmccaff/syllabi/CMSD%20320/362unit11.html>.
- [11] J.P. Mohr. A Randomized trial of Unruptured Brain Arteriovenous malformations (ARUBA). <http://www.arubastudy.org/main>, 2006.
- [12] Peter Nakaji, Pankaj Gore, and Robert F. Spetzler. Management of arteriovenous malformations: A surgical perspective. *Neurology India*, 53(1):14–16, 2005.
- [13] NYU Medical Center, Department of Neurosurgery. [http://www.med.nyu.edu/neurosurgery/subspecialty/cerebrovascular\\_2.html](http://www.med.nyu.edu/neurosurgery/subspecialty/cerebrovascular_2.html).
- [14] National Institute of Neurological Disorders and Stroke. Arteriovenous malformation information page. <http://www.ninds.nih.gov/disorders/avms/avms.htm>.
- [15] Christopher S. Ogilvy, Philip E. Stieg, Issam Awad, Robert D. Brown Jr, Douglas Kondziolka, Robert Rosenwasser, William L. Young, and George Hademenos. Recommendations for the management of intracranial arteriovenous malformations: A statement for healthcare professionals from a special writing group of the Stroke Council, American Stroke Association. *Circulation*, 103:2644–2657, 2001.
- [16] Mette S. Olufsen. Structured tree outflow condition for blood flow in larger systemic arteries. *Am J Physiol Heart Circ Physiol*, 276:257–268, 1999.
- [17] Mette S. Olufsen, Ali Nadim, and Lewis A. Lipsitz. Dynamics of cerebral blood flow regulation explained using a lumped parameter model. *Am J Physiol Regulatory Integrative Comp Physiol*, 282:R611–R622, 2002.

- [18] F.T. Smith and M.A. Jones. One-to-few and one-to-many branching tube flows. *J. Fluid Mech.*, 423:1–31, 2000.
- [19] F.T. Smith, N.C. Ovenden, P.T. Franke, and D.J. Doorly. What happens to pressure when a flow enters a side branch? *J. Fluid Mech.*, 479:231–258, 2003.
- [20] F.T. Smith, R. Purvis, S.C.R. Dennis, M.A. Jones, N.C. Ovenden, and M. Tadjfar. Fluid flow through various branching tubes. *Journal of Engineering Mathematics*, 47:277–298, 2003.
- [21] R.F. Spetzler and N.A. Martin. A proposed grading system for arteriovenous malformations. *J. Neurosurg.*, 65(4):476–483, 1986.
- [22] C. Stapf, J.P. Mohr, R.R. Sciacca, A. Hartmann, B.D. Aagaard, J. Pile-Spellman, and H. Mast. Incident hemorrhage risk of brain arteriovenous malformations located in the arterial borderzones. *Stroke*, 31:2365–2368, 2000.
- [23] Brooke N. Steele, Jing Wan, Joy P. Ku, Thomas J.R. Hughes, and Charles A. Taylor. In vivo validation of a one-dimensional finite-element method for predicting blood flow in cardiovascular bypass grafts. *IEEE Transactions on Biomedical Engineering*, 50(6):649–656, 2003.
- [24] StrokeSTOP, University of Massachusetts. <http://www.umassmed.edu/strokestop/>.
- [25] Charles A. Taylor, Mary T. Draney, Joy P. Ku, David Parker, Brooke N. Steele, Ken Wang, and Christopher K. Zarins. Predictive medicine: Computational techniques in therapeutic decision-making. *Computer Aided Surgery*, 4:231–247, 1999.
- [26] University of Toronto Brain Vascular Malformation Study Group. [http://www.brainavm.uhnres.utoronto.ca/malformations/brain.avm\\_index.htm](http://www.brainavm.uhnres.utoronto.ca/malformations/brain.avm_index.htm).
- [27] William L. Young, Abraham Kader, Isak Prohovnik, Eugene Ornstein, Lauren H. Fleischer, Noeleen Ostapkovich, LaSandra D. Jackson, and Bennett M. Stein. Pressure autoregulation is intact after arteriovenous malformation resection. *Neurosurgery*, 34(4):491–497, 1992.